Cellular Responses to Substrate Topography: Role of Myosin II and Focal Adhesion Kinase

Margo T. Frey,*† Irene Y. Tsai,‡ Thomas P. Russell,‡ Steven K. Hanks,§ and Yu-li Wang*
*Department of Physiology, University of Massachusetts Medical School, Worcester, Massachusetts 01605; †Department of Biomedical Engineering, Worcester Polytechnic Institute, Worcester, Massachusetts 01609; ‡Department of Polymer Science and Engineering, University of Massachusetts, Amherst, Massachusetts 01003; and §Department of Cell and Developmental Biology, Vanderbilt University School of Medicine, Nashville, Tennessee 37232

ABSTRACT Although two-dimensional cultures have been used extensively in cell biological research, most cells in vivo exist in a three-dimensional environment with complex topographical features, which may account for at least part of the striking differences between cells grown in vivo and in vitro. To investigate how substrate topography affects cell shape and movement, we plated fibroblasts on chemically identical polystyrene substrates with either flat surfaces or micron-sized pillars. Compared to cells on flat surfaces, 3T3 cells on pillar substrates showed a more branched shape, an increased linear speed, and a decreased directional stability. These responses may be attributed to stabilization of cell adhesion on pillars coupled to myosin II-dependent contractions toward pillars. Moreover, using FAK−/− fibroblasts we showed that focal adhesion kinase, or FAK, is essential for the responses to substrate topography. We propose that increased surface contact provided by topographic features guides cell migration by regulating the strength of local adhesions and contractions, through a FAK- and myosin II-dependent mechanism.

INTRODUCTION

Cell migration is essential for tissue development and homeostasis, including the responses to wounds and inflammation. Although cell migration on two-dimensional (2D) surfaces in vitro has been investigated in detail, migration in vivo is known to occur predominantly in a three-dimensional (3D) environment with complex physical, chemical, and topographical features. Compared to cells on 2D surfaces, cells in vivo or in model tissues show a drastically different morphology and behavior, including the lack of prominent stress fibers and focal adhesions (1–3).

Although most investigations have focused on chemical factors, accumulating evidence indicates that cells can respond to physical parameters such as substrate rigidity and mechanical stress, as well as topographic features such as grooves on the surface. Fibroblast migration may be directed toward increased substrate adhesivity (4), stiffness (5), or tension (5). In addition, on substrates inscribed with grooves, fibroblasts become highly elongated and crawl either inside or along the edge of grooves (depending on the depth of the groove; (6)), as if they were seeking maximal topographical stimulation. This phenomenon has been referred to as contact guidance (7). Recent observations further indicate that the dorsal-ventral asymmetry of substrate adhesion in 2D cultures plays a major role in stimulating cell spreading and stress fiber assembly. When both dorsal and ventral surfaces are anchored on the extracellular matrix (ECM), fibroblasts become elongated and show few large stress fibers, similar to what is found in connective tissues (3).

Despite the long awareness of contact guidance, there has been only limited knowledge of how cells detect and respond to topographic features. There are strong indications that integrins and focal adhesions play a major role in the responses to nonchemical stimuli. Focal adhesions, associated with the actin cytoskeleton on the cytoplasmic side and the ECM on the extracellular side, are the exertion points of cellular contractile forces on the substrate. The cytoplasmic face of the focal adhesion is also known to carry a complex battery of structural (e.g., vinculin, α-actinin, and paxillin) and signaling proteins (e.g., focal adhesion kinase, or FAK, and src) (8). Although the exact functions of these signaling molecules are unclear, they presumably play the important role of transmitting extracellular physical or topographic signals across the membrane and translating them into intracellular chemical or physical signals. Consistent with this idea, cells in some late-stage tumors show overexpression of FAK (9–13), whereas FAK−/− and myosin IIB−/− fibroblasts are also defective in their responses to mechanical stimulations (14,15).

Although grooved substrates have been used extensively for studying cellular responses to topographic signals (6,16–18), the exclusive localization of cells within the grooves and the extremely narrow width impede the investigation into the migration responses and structural organization. We have therefore designed polystyrene substrates that contain a field of semiordered, micron-sized pillars, such that migrating cells continuously encounter alternating flat and bumpy surfaces. Comparison with cells on flat polystyrene surfaces allowed us to determine unambiguously the responses to

Submitted September 15, 2005, and accepted for publication February 6, 2006.

Address reprint requests to Yu-li Wang, PhD, University of Massachusetts Medical School, 377 Plantation Ave., Suite 327, Worcester, MA 01605. Tel.: 508-856-8781; Fax: 508-856-8774; E-mail: yuli.wang@umassmed.edu.

0006-3495/06/05/3774/09 $2.00

doi: 10.1529/biophysj.105.074526

topographical features. This strategy has provided not only new insights into how normal fibroblasts respond to substrate topography, but also a powerful test for the requirements of specific proteins. Our results suggest that substrate topography guides cell migration by enhancing the stability of adhesions at pillars coupled to myosin II-dependent contractions. In addition, we demonstrate that FAK is essential for these responses.

MATERIALS AND METHODS

Preparation and characterization of substrates

To generate the pillar topography, polymethylmethacrylate was applied to a silicon oxide surface and subjected to a strong electric field as described elsewhere (19,20). Electrohydrodynamic instabilities caused the surface to form micron-sized pillars. Polydimethylsiloxane was then poured over the pillars and cured overnight at 60°C to serve as the template. The template was then pressed onto a 1-μm thick polystyrene film at 150°C atop a coverslip and peeled off. This simple approach generated a semiordered array of pillars on part of the polystyrene surface. The surfaces were then made hydrophilic by reactive ion etching.

Topographical images of the substrate (Fig. 1) were obtained using an Autoprobe M4 atomic force microscope (AFM) (Veeco, Santa Barbara, CA) equipped with ProScan V1.51b software (Veeco). Images were acquired in contact mode with a standard tipped CSC12 cantilever of 0.03 N/m nominal stiffness (Veeco). Dimensions of the pillars were determined from AFM images collected on three different samples. All observations reported here were made in regions with a similar size, density, and distribution of the pillars. Typical pillars are 1.78 $\pm$ 0.02 μm in height, 10.30 $\pm$ 0.19 μm in diameter, and are spaced 15.76 $\pm$ 0.26 μm center-to-center (mean $\pm$ SE, $n = 33$ for each). Assuming a regular distribution of pillars on a grid, we estimated that ~46% of the total surface is located on the top and side of pillars, and ~54% as flat surfaces between the pillars.

Coverslips carrying the polystyrene substrate were mounted onto 35-mm cell culture dishes (Falcon, Nowhere, NV), with a hole drilled at the center, using ultraviolet-cured optical adhesive (Type 71, Norland Products, Cranbury, NJ). Before use, culture dishes containing the substrates were sterilized by exposure to ultraviolet light inside a cell culture hood for 10 min.

Cell culture and transfection

All cells were maintained in a standard incubator with 5% CO_2. Experiments were performed within 3 days of plating onto topographical substrates. NIH 3T3 fibroblasts were obtained from Dr. Ann F. Chambers, University of Western Ontario, London, Ontario, Canada (1,21) and were cultured in Dulbecco's modified Eagle medium (Sigma, St. Louis, MO) containing 10% donor calf serum (Hyclone, Logan, UT) supplemented with 10,000 units/ml penicillin, 10,000 μg/ml streptomycin, and 29.2 mg/ml L-glutamine for up to 20 passages. FAK−/− fibroblasts reexpressing FAK under Tef-off control have been described previously (22). The cells were cultured in Dulbecco's modified Eagle medium (Sigma) containing 10% fetal bovine serum (Atlanta Biologicals, Norcross, GA) supplemented with 10,000 units/ml penicillin, 10,000 μg/ml streptomycin, 29.2 mg/ml L-glutamine, and 1% nonessential amino acids (GIBCO/BRL, Grand Island, NY). Tetracycline (Calbiochem, San Diego, CA) was added during each change of media at a concentration of 1 μg/ml to prevent expression of the FAK protein in FAK−/− experiments. To induce FAK expression, the same FAK−/− cells were transferred to media lacking tetracycline for 36–48 h before experiments (22). To image focal adhesions, cells were transfected with plasmids carrying enhanced green fluorescent protein (EGFP) tagged paxillin (23), using the Amaxa nucleofector and kit R following the protocol recommended by the manufacturer (Amaxa, Gaithersburg, MD). Cells were plated onto the substrates at a low density to minimize cell-cell contacts.

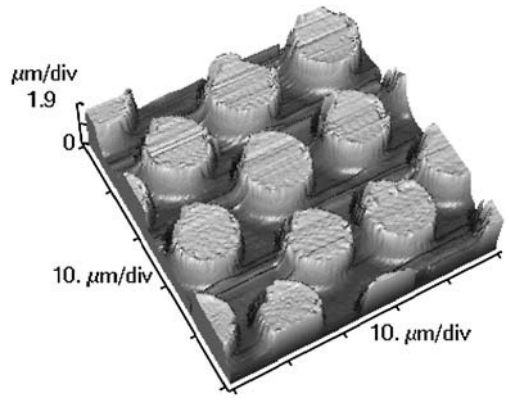

FIGURE 1 Topography of pillar substrate. Topographical images of pillar substrates were taken by AFM in contact mode. A 50- × 50-μm region is shown as a projected three-dimensional image. Fine features on top of the pillars are likely an imaging artifact.

Blebbistatin (Toronto Research Chemicals, Ontario, Canada), an inhibitor of nonmuscle myosin II ATPase (24,25), was applied by replacing the culture medium with medium containing 100 μM blebbistatin as described previously (26). Experiments were performed after 2 h of incubation. Because blebbistatin is sensitive to blue light (27,28), a red filter was placed in the transmission illumination light path during image acquisition, and the total period of data acquisition was limited to within 8 h.

Video microscopy and cell motility measurements

Cell-plated substrates were loaded into a stage incubator on a Zeiss (Jena, Germany) IM35 microscope equipped with a Neo-Fluar 25× N.A. 0.8 oil phase objective lens. Images were acquired with a video rate surveillance charge-coupled device (CCD) camera (Mintron 12V1E-EX, Santa Clara, CA) or with a Roper NTE/CCD-512-EBFT camera (Roper Scientific, Trenton, NJ). Time-lapse images were recorded every 2–4 min for a period of at least 2 h and analyzed with custom software. Cells selected for analysis were spread, motile, separated from neighboring cells, and were neither exiting nor entering mitosis. Additionally, all the quantitative analyses were performed in regions of similar pillar size and density. Coordinates of the nuclear centroid were determined automatically using a pattern recognition algorithm. Because double-reciprocal analysis as applied previously did not generate straight lines for cells on pillar substrates (14,29), linear speed (S, in μm/min) was calculated by simply dividing the integrated travel distance with the total time T (Eq. 1, where x_i and y_i are coordinates at frame i).

$$S = (\Sigma\sqrt{((x_i - x_{i-1})^2 + (y_i - y_{i-1})^2)})/T. \quad (1)$$

Note that this approach is unaffected by the turning behavior whereas the previous approach based on mean squared displacements is sensitive to migration pattern (14). Average acceleration of velocity (A, in μm/min^2, Eq. 2) was calculated based on changes in the distance of travel along x- and y-directions between three consecutive frames.

$$A = (\Sigma\sqrt{(((x_i - x_{i-1}) - (x_{i-1} - x_{i-2}))^2 + ((y_i - y_{i-1}) - (y_{i-1} - y_{i-2})^2)}))/T^2. \quad (2)$$

A turn was defined as a change in direction of at least 30° between two consecutive intervals of recording with a distance of at least 2.0 μm in the intervals following the change in direction. The total number of turns for each series was then divided by the recording time to yield average turns per hour. Unpaired Student's t-tests were performed using GraphPad software and all data represented as mean $\pm$ SE unless otherwise indicated. Average lifespan of focal adhesions was determined using cells transfected with EGFP-paxillin, as the length of time between the appearance and

disappearance of an adhesion (30). The average was calculated from 27 focal adhesions in four cells in each group.

Cell fixation and staining

Cells were rinsed twice with 37°C phosphate buffer saline (PBS), and fixed with 4% paraformaldehyde (Electron Microscopy Sciences, Fort Washington, VA) and 0.2% Triton X-100 (Sigma) in PBS for 10 min. After rinsing twice in PBS with 1% bovine serum albumin (Sigma) for 10 min each, focal adhesions were stained with a monoclonal anti-vinculin antibody (1:100 dilution; Sigma), and Alexa-546 goat anti-mouse secondary IgG (1:100 dilution, Molecular Probes, Eugene, OR). Cells were counterstained with Alexa-488 phalloidin (Molecular Probes) to visualize actin filaments, following the manufacturer's instructions.

Fluorescent images were obtained using a Zeiss Axiovert-10 microscope with a Roper NTE/CCD-512-EBFT camera. A Zeiss Fluar 100× N.A. 1.30 phase objective lens was used to acquire fluorescence images as optical slices at a distance interval of 0.25 μm. Images were deconvolved using a constrained iterative algorithm using custom software. In addition, low-magnification fluorescence images, along with phase contrast images, were collected with a Neo-Fluar 40× N.A. 0.75 lens for morphometry. Cellular processes, defined as nonoverlapping, vinculin plaque-containing regions of the cell boundary where the distance from cell center is longer than both neighboring regions, were determined from phalloidin and vinculin images. The perimeter, p, of each cell was traced by hand on phalloidin-stained images and the spread area, A, computed based on the number of pixels within the perimeter. Form factor, a measure of the degree of branching in cell shape, was then calculated as $4\pi A / p^2$. Cells with a spread area between 485 and 1725 μm^2 were included in the analysis of cellular processes and form factor, to exclude rounded or abnormally large cells.

Fibronectin adsorption and characterization

To determine if fibronectin (FN) in the media was adsorbed uniformly over the surface of pillar substrates, FN was fluorescently labeled and the relative intensities on top and in between pillars were compared. Substrates were incubated overnight in the medium used for 3T3 cells, rinsed and incubated twice with 37°C PBS with 1% bovine serum albumin (Sigma) for 10 min each, and then labeled sequentially with a monoclonal anti-FN antibody (1:100 dilution; Sigma), and Alexa-488 goat anti-mouse secondary IgG (1:100 dilution, Molecular Probes) for 45 and 30 min, respectively. Fluorescent images were acquired as described above with a Fluar 100× N.A. 1.30 phase objective lens. Intensities measured on top and in between pillars ($n = 50$ for each from two substrates) were corrected by subtracting average background fluorescence measured on similar substrates prepared without the primary antibody.

RESULTS

Pillar topography induces branched morphology and erratic movement of 3T3 fibroblasts

To create substrates with topographic features, coverslips were coated with polystyrene and pillar features were cast on part of the surface using polydimethylsiloxane molding (see Materials and Methods). The topographic feature consisted of cylindrical pillars that are on average 1.78 μm in height, 10.30 μm in diameter, and 15.76 μm in center-center spacing as determined by atomic force microscopy (Fig. 1). The entire substrate was then modified by reactive ion etching to promote cell adhesion. The resulting surfaces were chemically similar to that of conventional polystyrene tissue culture dishes. Flat and pillar regions shared identical chemical properties and differed only in topographical features. Quantitative immunofluorescence indicated that the surface was coated similarly with FN on top of the pillars and in the flat region between pillars (relative intensities of 49.9 ± 2.4 on top of pillars and 48.1 ± 1.6 in between pillars, p-value = 0.592).

NIH 3T3 fibroblasts on pillar substrates were able to follow the topography and form focal adhesions on the top and sides of the pillars, and in the flat regions between pillars (Fig. 2 and supplemental Video 1 in Supplementary Material). Compared to those on the flat substrates, focal adhesions on pillar substrates appeared smaller in size (Fig. 2). In addition, cells on pillars appeared to be more branched in shape (Fig. 3,

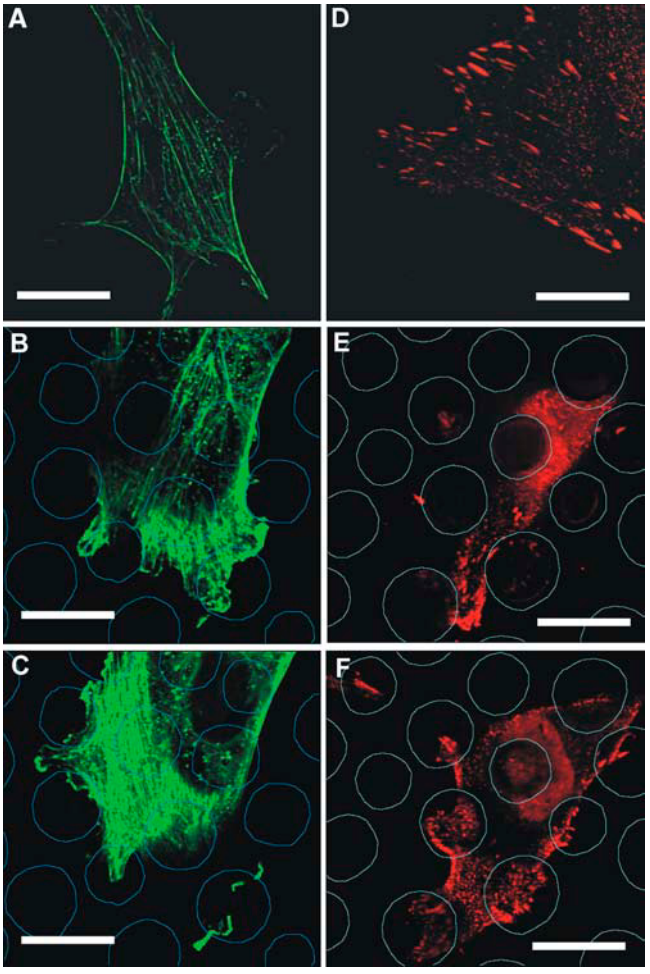

FIGURE 2 Focal adhesions and stress fibers in NIH 3T3 cells on pillar and flat substrates. NIH 3T3 cells on flat (*A* and *D*), or pillar (*B*, *C*, *E*, and *F*) substrates were fixed and stained for actin filaments (*A–C*), or vinculin (*D–F*). Optical sections were deconvolved and partially reconstructed to show structures in the upper (*C* and *F*), or lower half (*B* and *E*), of the cell. Pillars were indicated as circles. On pillar substrates, focal adhesions form both on pillars and on the flat surface between pillars. In addition, cells appeared to form more prominent focal adhesions on flat substrates than on pillar substrates. Bar, 20 μm. See also supplemental Videos 1 and 2.

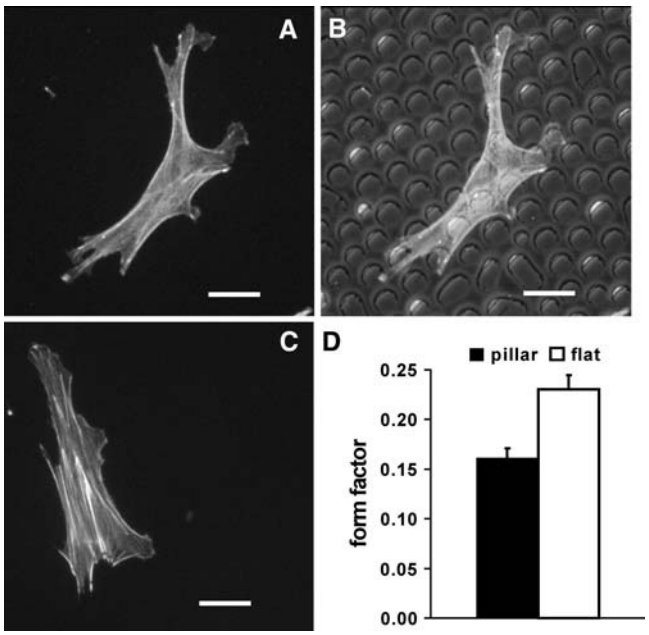

FIGURE 3 Morphology of NIH 3T3 cells on pillar and flat substrates. Phalloidin staining shows a more branched morphology for cells on pillar substrate (*A* and *B*), than cells on flat substrate (*C*). Images of phalloidin and vinculin were merged (*A* and *C*), then merged with phase contrast image to show the location of pillars (*B*). Bar, 20 μm. Shape complexity is quantified by calculating the form factor (*D*); more branched shape yields a smaller form factor. Bars represent mean ± SE for 33 cells under each condition.

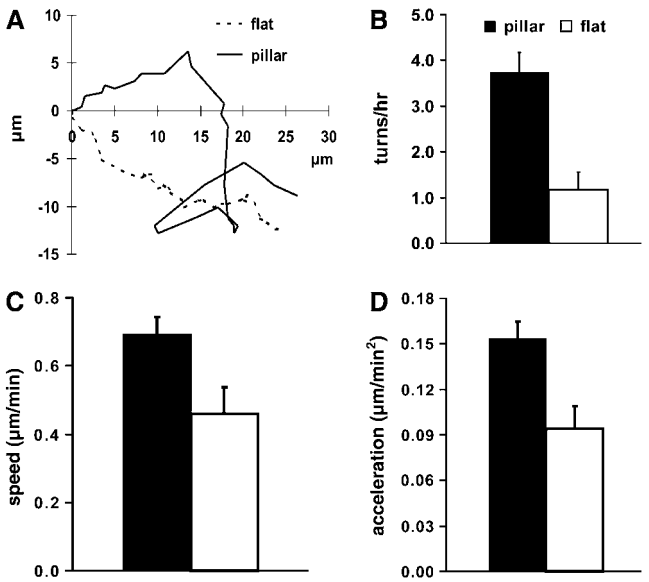

FIGURE 4 Migration characteristics of NIH 3T3 cells on pillar and flat substrates. Representative paths of cell migration, as determined by tracing the nuclear centroid over a period of 2 h, show a longer, more zigzag path on pillar substrate (*A*, *solid line*), than on flat substrate (*A*, *dotted line*). The differences are quantified by measuring the turning frequency (*B*), the linear speed (*C*), and vectorial acceleration (*D*). Compared to cells on flat substrates, those on pillar substrates show a significantly higher turning frequency (*B*, *solid bar*), linear speed (*C*, *solid bar*), and vectorial acceleration due to frequent changes in direction (*D*, *solid bar*). Bars represent mean ± SE for eight cells (*B*, *C*, and *D*). See also supplemental Videos 3–5.

A–C), as confirmed by measuring the form factor (defined as 4π area / perimeter^2; more convoluted shapes show a longer perimeter relative to the area, thus a smaller form factor). We obtained a value of 0.161 ± 0.010 for cells on pillar substrate and 0.230 ± 0.014 for cells on the flat region (p-value = 0.0001, Fig. 3 *D*), confirming that cells on pillar substrates have a more complex shape.

We noticed that branches of the cell appeared to associate preferentially with pillars (Fig. 3 *B*). Quantitative analysis of fluorescently stained cells confirmed that vinculin-containing cellular processes were twice as likely to terminate at pillars as in the region between pillars (66.9% vs. 33.1% from 25 cells), even though pillars account for only ~46% of the total surface area. These observations may be explained if pillars promote stable cell adhesion.

The branched morphology and the preferential association of cellular processes with pillars suggest that pillar topography may affect cell migration. We found that cells on pillar substrates moved in a zigzag fashion, as if they were dragged from pillar to pillar by the anchored extensions (Fig. 4 *A* and supplemental Videos 3 and 4). Quantification of the frequency of turns confirmed this observation (3.74 ± 0.43 vs. 1.17 ± 0.39 turns per hour for pillar and flat substrates, respectively, p-value = 0.0006, Fig. 4 *B*). Measurements of cell movement indicated that cells on pillar substrates moved at a significantly higher linear speed than those on flat regions (0.692 ± 0.051 vs. 0.459 ± 0.077 μm/min, respectively, p-value = 0.0246; Fig. 4 *C* and supplemental Videos 3–5). The irregular movement was further supported by measuring the vectorial acceleration, which decreased from 0.153 ± 0.011 μm/min^2 on pillars to 0.094 ± 0.015 μm/min^2 on flat substrates (p-value = 0.0071; Fig. 4 *D*) due to less frequent changes in direction on flat substrates (Fig. 4, *A* and *B*).

Responses to pillar topography involve stabilization of focal adhesions and myosin II-dependent contractility

The preferential association of cellular processes with pillars and the erratic pattern of cell movement suggest that the pillar topography promotes stable cell adhesion. To address this possibility, we measured the turnover of focal adhesions on pillar and flat surfaces, using NIH 3T3 cells transfected with EGFP-paxillin to label focal adhesions (23). The average lifespan of focal adhesions on pillars was 40.74 ± 4.01 min, compared to 21.11 ± 0.98 min for those on flat surfaces between pillars (p-value < 0.0001, Fig. 5), indicating that topographic features increase the stability of focal adhesions.

The zigzag migration pattern on pillar substrates further suggests that contractile forces may play a role, by dragging cells from pillar to pillar. To determine if myosin II is involved

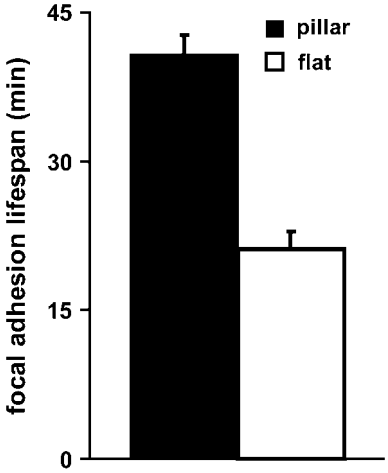

FIGURE 5 Stability of focal adhesions on pillar and flat substrates. Average life span of focal adhesions, determined using NIH 3T3 cells expressing EGFP-paxillin, indicates a higher stability for focal adhesions on pillars than for those on the flat surface between pillars. Bars represent mean ± SE for 20–30 focal adhesions in four cells under each condition.

in this process, we treated cells with blebbistatin, a potent inhibitor of nonmuscle myosin II ATPases (25). Blebbistatin-treated cells showed a highly elongated, irregular morphology independent of substrate topography (Fig. 6, *A* and *B*). Although the cells remained motile, neither the linear speed (0.384 ± 0.028 vs. 0.408 ± 0.052 μm/min for pillar and flat, respectively, p-value = 0.6943; Fig. 6 *C*), nor the vectorial acceleration (0.111 ± 0.008 vs. 0.099 ± 0.012 μm/min for pillar and flat, respectively, p-value = 0.3523; Fig. 6 *D*), responded to the pillar topography (supplemental Video 6). These results suggest that myosin II provides the driving forces for the detection and/or responses of 3T3 cells to substrate topography.

Responses to substrate topography require FAK

We demonstrated previously that FAK is required for cellular responses to mechanical stimulation (14). To determine if FAK is required for the responses to substrate topography, we analyzed time-lapse images of FAK−/− fibroblasts reexpressing FAK under the control of a Tet-off system. FAK expression was inhibited when cells were cultured in the presence of tetracycline. Removal of tetracycline for 36–48 h induced reexpression of FAK (22).

Rescued cells responded to the pillar topography in a similar manner as did NIH 3T3 cells. The extensions showed a preferential association to pillars, as 61.1% of processes terminated on pillars versus 38.9% in between pillars (data from 24 cells, Fig. 7 *A*), and an increased frequency of turns on pillar substrates (5.14 ± 0.43 vs. 2.34 ± 0.28 turns per hour for pillar and flat substrates, respectively, p-value = 0.0001; Fig. 8, *A*, *B*, and *E*, and supplemental Videos 7 and 8). As for 3T3 cells, rescued cells showed a lower form factor

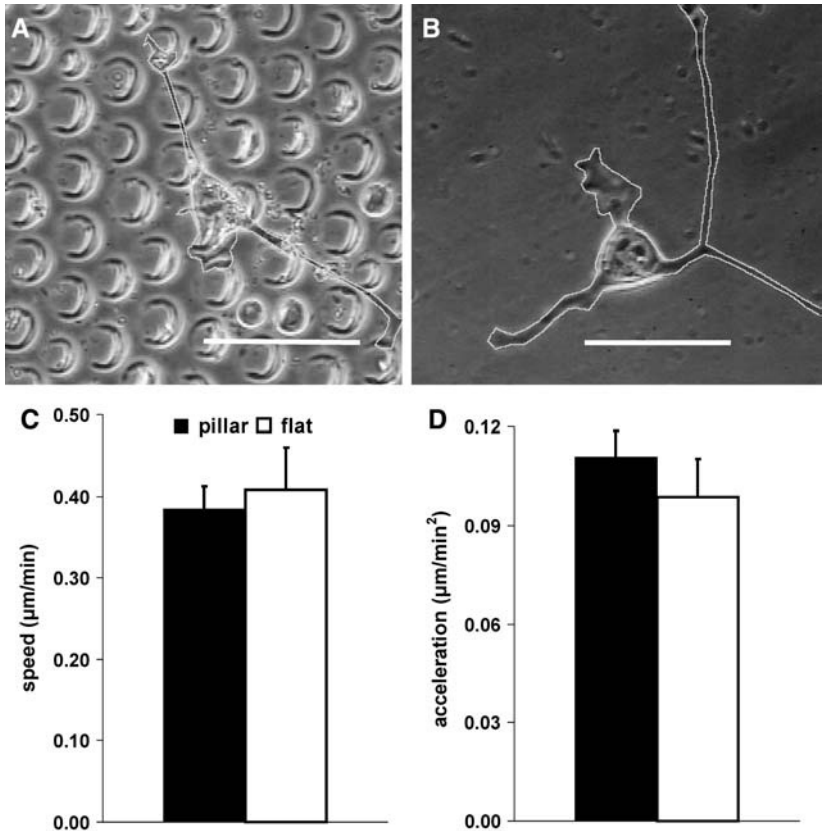

FIGURE 6 Effect of myosin inhibitor on NIH 3T3 cells plated on pillar and flat substrates. Cells are treated with 100 μM blebbistatin for at least 2 h before imaging. Approximate boundaries, drawn for clarity due to poor contrast relative to pillars, show a similar elongated and irregular shape on pillar (*A*) and flat (*B*) substrate. Bar, 50 μm. Linear speed (*C*) and vectorial acceleration (*D*), calculated as for Fig. 4, also show statistically similar values. Bars represent mean ± SE calculated for eight cells under each condition. See also see supplemental Video 6.

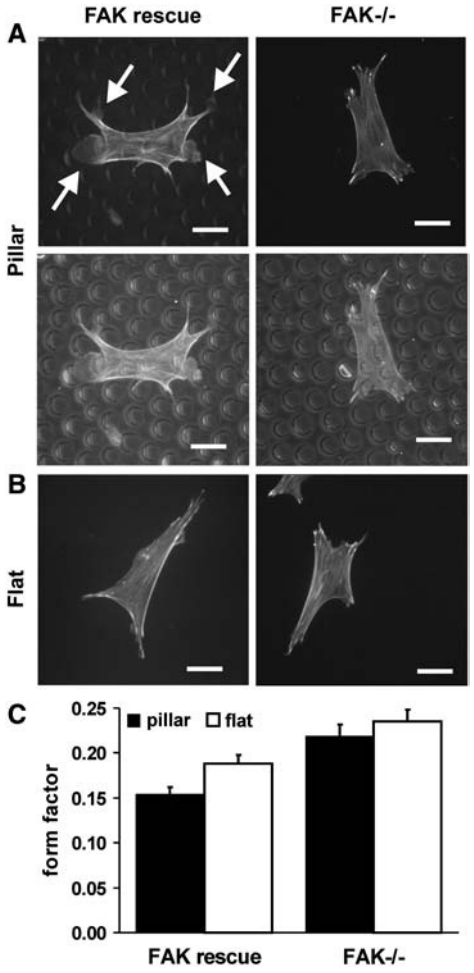

FIGURE 7 Morphology of FAK−/− and rescued cells on pillar and flat substrates. Phalloidin staining shows a more convoluted shape for rescued cells on pillar substrate (*A*), than on flat substrate (*B*), whereas FAK−/− cells show a similar simple shape on both substrates. In addition, FAK−/− cells show reduced ruffling activities on either pillar or flat substrate compared to FAK-expressing cells (*A*, *arrows*). Distribution of the pillars is shown in the merged fluorescence and phase contrast images (*A*, *bottom row*). Bar, 20 μm. Shape complexity, quantified by the form factor (*C*), indicates that FAK−/− cells fail to respond to the pillars whereas rescued cells show statistically significant responses similar to NIH 3T3 cells. Bars represent mean ± SE for 33 cells under each condition.

(0.155 ± 0.008 vs. 0.188 ± 0.010, p-value = 0.0094; Fig. 7 *C*), higher linear speed (0.870 ± 0.109 vs. 0.394 ± 0.024 μm/min, p-value = 0.0008; Fig. 8 *C* and supplemental Videos 7 and 8), and higher vectorial acceleration (0.263 ± 0.032 vs. 0.102 ± 0.005 μm/min^2, p-value = 0.0002; Fig. 8 *D* and supplemental Videos 7 and 8), on pillar than on flat substrates. In addition, compared to rescued cells on flat substrates, those on pillars displayed a greater number of extensions, most of which terminated at a small ruffling region on a pillar (Fig. 7 *A*).

In contrast to rescued cells, FAK−/− cells showed no detectable response to the pillar topography (Fig. 7 *A*). Comparisons of migration paths indicated a similar pattern on the pillar and flat substrates (Fig. 8, *A* and *F*), confirmed by the similar turning frequency (2.44 ± 0.34 vs. 2.04 ± 0.31 turns per hour for pillar and flat substrates, respectively, p-value = 0.4017, Fig. 8 *B*). In addition, cellular processes showed a reduced tendency to terminate at pillars (48.9% vs. 51.1% for pillar and between pillars from 25 cells). The form factor (0.219 ± 0.013 vs. 0.235 ± 0.013, p-value = 0.3834; Fig. 7 *C*), linear speed (0.427 ± 0.044 vs. 0.471 ± 0.028 μm/min, p-value = 0.4248; Fig. 8 *C*), and vectorial acceleration (0.137 ± 0.017 vs. 0.108 ± 0.008 μm/min^2, p-value = 0.1479; Fig. 8 *D*) all remained similar on pillar and flat substrates. The linear speed of FAK−/− cells was similar to that for FAK rescued cells on flat substrates (0.394 ± 0.024 vs. 0.471 ± 0.028 μm/min, p-value = 0.0553, Fig. 8 *C*; to be distinguished from root mean squared displacement based speed (14), see Materials and Methods) (31,32). FAK−/− cells also showed a less convoluted shape and lower ruffling activities than rescued cells on flat surfaces (form factor of 0.235 ± 0.013 vs. 0.188 ± 0.010, p-value = 0.0052; Fig. 7, *A* and *C*).

DISCUSSION

Although the phenomenon of contact guidance has been known for decades (7), the mechanism of cellular responses to substrate topography remains poorly understood. Pillar substrates allow migrating cells to continuously encounter localized topographic stimuli, and facilitate direct comparison of cell behavior on surfaces with or without topographic features. Compared to cells on flat surfaces, 3T3 cells on pillar substrates showed a more branched shape, increased linear speed, and decreased directional stability. The pillars appeared to serve as preferred sites for ruffling activities and anchorage, as extensions of 3T3 fibroblasts were more than twice as likely to terminate at a pillar than in between pillars at a given time, even though the pillar surface area accounted for less than one-half of the total surface area.

Observations of focal adhesions and blebbistatin treatment provided mechanistic insights into the responses to topographic signals. Stable association at pillars was likely caused by localized stabilization of focal adhesions, as shown by the decrease in the turnover rate of focal adhesions on pillars from that on flat regions between pillars. Anchorage to pillars was typically followed by contractions of the cell extension, causing acceleration toward the pillars and abrupt changes in direction. This enhanced contraction may account for the increase in linear speed despite the increased stability of focal adhesions. In addition, inhibition of the responses to surface topography by blebbistatin suggests that myosin-II-dependent contraction plays a role in the process, possibly by providing forces for the cell to surge toward stabilized adhesions at pillars. Similar combinations of localized enhancement of adhesions and contractions would readily explain cellular responses to other topographic features,

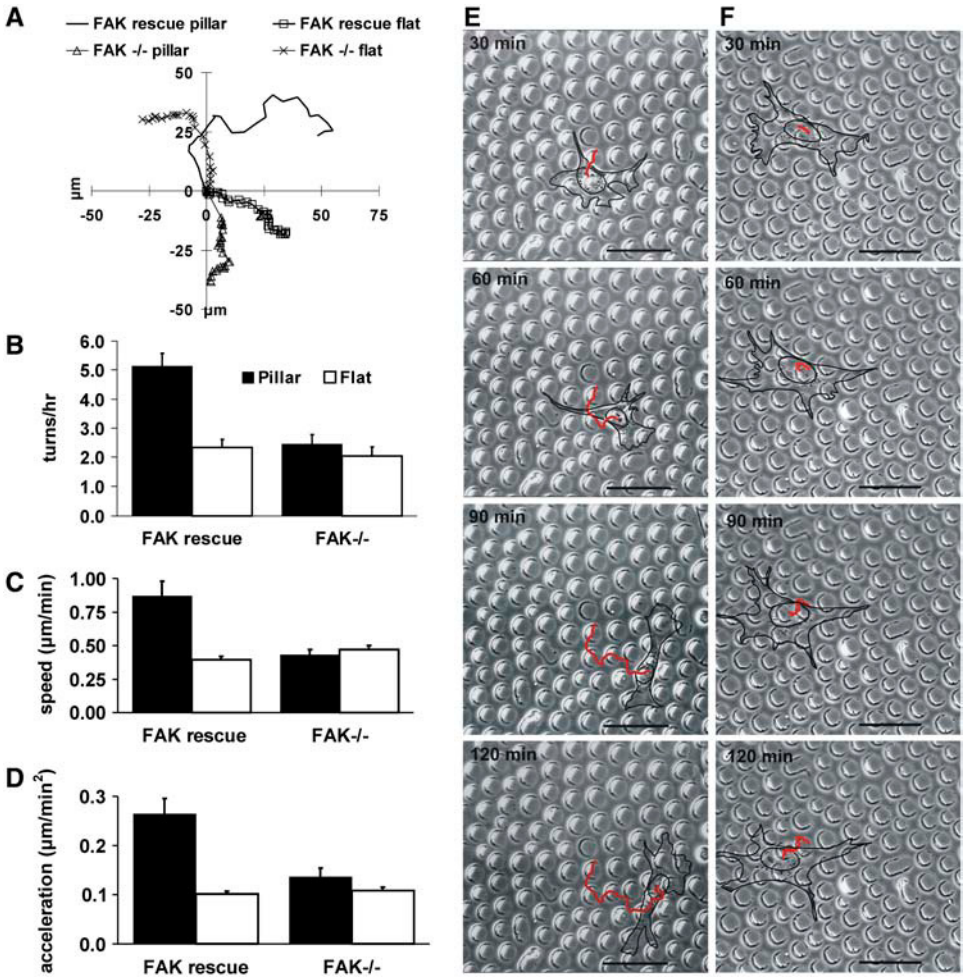

FIGURE 8 Migration characteristics of FAK−/− and rescued cells on flat and pillar substrates. (*A*) Migration patterns of representative cells (chosen based on linear speed) indicate that rescued cells move in a more zigzag pattern on pillar substrates than on flat substrates, unlike the similar migration patterns of FAK−/− cells on pillar and flat substrates. Quantification of turns confirms these observations (*B*). In addition, linear speed (*C*) and vectorial acceleration (*D*) of FAK−/− cells fail to respond to the pillars, whereas those of rescued cells respond in a way similar to 3T3 cells. Linear speed and vectorial acceleration for FAK−/− and rescued cells are analyzed as for 3T3 cells shown in Fig. 4. Bars represent mean ± SE for eight cells under each condition. Representative sequences of phase contrast images for rescued (*E*), and FAK−/− cells (*F*), on pillar substrates also show a lack of turning responses to pillars for FAK−/− cells. Due to low contrast on pillar substrates, approximate cell boundaries are traced in black and migration paths indicated in red. Bar, 50 μm. See also supplemental Videos 7 and 8.

including the alignment with grooves in classic contact guidance.

The response to surface topography may involve responses to surface curvature or to increased substrate contact area. However, since grooves and ridges, and pits and pillars, were previously found to induce similar responses (6,16–18,33), the sign of the curvature does not appear to play an important role. Instead, it is probably the density of anchored surface receptors relative to cell volume that is responsible for the stimulation. Interestingly, large pits and/or spacing were reported to inhibit cell migration (33). This may be explained if cells were unable to straddle multiple pillars or pits under these conditions, such that strong anchorage to single topographic features may limit the ability of cells to migrate onto the surrounding flat surface.

The responses to surface topography appear very similar to the responses to substrate rigidity. We have shown that fibroblasts exert stronger traction forces on stiff substrates than on soft substrates (5). Moreover, cells also adhere more tightly to stiff substrates than to soft substrates, as shown by a centrifugation assay and by a microneedle peeling assay (34,35). Similar increases in cellular spreading, migration speed, and traction forces were reported in response to increases in collagen surface density (36). Thus, mechanical and topographic signals may elicit similar responses, causing cells to steer toward maximal stimulation through enhancements of anchorage and contraction.

Although detailed mechanism for the transduction of such topographic or physical signals is unclear, one possibility is that mechanical forces transmitted through integrins may cause an associated sensing protein on the cytoplasmic side to change its conformation and enzyme/substrate activities. Mechanical forces are also known to cause calcium entry through ubiquitous stretch-sensitive channels, and activate a number of potential downstream effectors including calmodulin and myosin II (37,38). Topographic features may induce similar responses, by increasing the density of local contacts and associated signals relative to the cell volume.

Although FAK has been recognized as a key enzyme in regulating cell migration (39), its functional role remains poorly defined. We showed that cellular responses to surface topography require FAK. The cell shape, linear speed, and migration pattern for FAK−/− cells were similar on flat and pillar substrates, as if FAK−/− cells were blind to the

presence of pillars. Consistent with this idea, we reported previously that FAK−/− cells lacked the response to substrate stiffness (14). Furthermore, we observed limited lamellipodia formation in FAK−/− cells on both flat and pillar substrates, whereas FAK-expressing cells showed localized enhancement of ruffling activities on pillars (unpublished data). Cells treated with siRNA against FAK showed a similar reduction in ruffling activities, suggesting that FAK is required for the activation of membrane protrusion and cell polarity (32). These observations indicated that FAK is involved in the detection of adhesion-mediated physical signals, possibly by amplifying the cytoplasmic chemical responses.

The physiological role of micron-scaled topographic signals remains largely unexplored in vivo. These signals may be created by aggregation or fibrillar assembly of ECM proteins. In addition, topographic signals may arise as a result of cell shape changes or cell-cell interactions. As demonstrated in this and previous studies with FAK−/− cells (14), defects in responses to mechanical or topographic signals may lead to relatively minor phenotypes when cells were examined under conventional culture conditions, but severe consequences under conditions where these signals play a major role such as during embryonic development or wound healing. Given the profound effects on cell shape, adhesion, and migration, topographic features also represent an important factor in the engineering of artificial tissues and prosthetic devices.

SUPPLEMENTARY MATERIAL

An online supplement to this article can be found by visiting BJ Online at http://www.biophysj.org.

We thank Dr. Juergen Wehland for providing the EGFP-paxillin plasmids, Dr. Nancy Burnham for use of the atomic force microscope, and Mr. Gregory Chua for technical assistance.

This project was supported by the National Institutes of Health (grant GM-32476 to Y-L.W and grant GM-49882 to S.H.), the Department of Energy's Office of Basic Energy Science, and the Materials Research Science and Engineering Center at the University of Massachusetts, sponsored by the National Science Foundation.

REFERENCES

1. Bondy, G. P., S. Wilson, and A. F. Chambers. 1985. Experimental metastatic ability of H-ras-transformed NIH3T3 cells. *Cancer Res.* 45:6005–6009.
2. Cukierman, E., R. Pankov, and K. M. Yamada. 2002. Cell interactions with three-dimensional matrices. *Curr. Opin. Cell Biol.* 14:633–639.
3. Beningo, K. A., M. Dembo, and Y. L. Wang. 2004. Responses of fibroblasts to anchorage of dorsal extracellular matrix receptors. *Proc. Natl. Acad. Sci. USA.* 101:18024–18029.
4. Carter, S. B. 1967. Haptotaxis and the mechanism of cell motility. *Nature.* 213:256–260.
5. Lo, C. M., H. B. Wang, M. Dembo, and Y. L. Wang. 2000. Cell movement is guided by the rigidity of the substrate. *Biophys. J.* 79:144–152.
6. Walboomers, X. F., W. Monaghan, A. S. Curtis, and J. A. Jansen. 1999. Attachment of fibroblasts on smooth and microgrooved polystyrene. *J. Biomed. Mater. Res.* 46:212–220.
7. Weiss, P. *Nerve patterns: the mechanics of nerve growth.* in *Third Growth Symposium.* 1941.
8. Geiger, B., A. Bershadsky, R. Pankov, and K. M. Yamada. 2001. Transmembrane crosstalk between the extracellular matrix-cytoskeleton crosstalk. *Nat. Rev. Mol. Cell Biol.* 2:793–805.
9. Rovin, J. D., H. F. Frierson Jr., W. Ledinh, J. T. Parsons, and R. B. Adams. 2002. Expression of focal adhesion kinase in normal and pathologic human prostate tissues. *Prostate.* 53:124–132.
10. Weiner, T. M., E. T. Liu, R. J. Craven, and W. G. Cance. 1994. Expression of growth factor receptors, the focal adhesion kinase, and other tyrosine kinases in human soft tissue tumors. *Ann. Surg. Oncol.* 1:18–27.
11. Tremblay, L., W. Hauck, A. G. Aprikian, L. R. Begin, A. Chapdelaine, and S. Chevalier. 1996. Focal adhesion kinase (pp125FAK) expression, activation and association with paxillin and p50CSK in human metastatic prostate carcinoma. *Int. J. Cancer.* 68:164–171.
12. Owens, L. V., L. Xu, R. J. Craven, G. A. Dent, T. M. Weiner, L. Kornberg, E. T. Liu, and W. G. Cance. 1995. Overexpression of the focal adhesion kinase (p125FAK) in invasive human tumors. *Cancer Res.* 55:2752–2755.
13. Cance, W. G., J. E. Harris, M. V. Iacocca, E. Roche, X. Yang, J. Chang, S. Simkins, and L. Xu. 2000. Immunohistochemical analyses of focal adhesion kinase expression in benign and malignant human breast and colon tissues: correlation with preinvasive and invasive phenotypes. *Clin. Cancer Res.* 6:2417–2423.
14. Wang, H. B., M. Dembo, S. K. Hanks, and Y. Wang. 2001. Focal adhesion kinase is involved in mechanosensing during fibroblast migration. *Proc. Natl. Acad. Sci. USA.* 98:11295–11300.
15. Lo, C. M., D. B. Buxton, G. C. Chua, M. Dembo, R. S. Adelstein, and Y. L. Wang. 2004. Nonmuscle myosin IIb is involved in the guidance of fibroblast migration. *Mol. Biol. Cell.* 15:982–989.
16. Curtis, A. S., B. Casey, J. O. Gallagher, D. Pasqui, M. A. Wood, and C. D. Wilkinson. 2001. Substratum nanotopography and the adhesion of biological cells. Are symmetry or regularity of nanotopography important? *Biophys. Chem.* 94:275–283.
17. Wojciak-Stothard, B., Z. Madeja, W. Korohoda, A. Curtis, and C. Wilkinson. 1995. Activation of macrophage-like cells by multiple grooved substrata. Topographical control of cell behaviour. *Cell Biol. Int.* 19:485–490.
18. Clark, P., P. Connolly, A. S. Curtis, J. A. Dow, and C. D. Wilkinson. 1990. Topographical control of cell behaviour. II. Multiple grooved substrata. *Development.* 108:635–644.
19. Morariu, M. D., N. E. Voicu, E. Schaffer, Z. Lin, T. P. Russell, and U. Steiner. 2003. Hierarchical structure formation and pattern replication induced by an electric field. *Nat. Mater.* 2:48–52.
20. Schaffer, E., T. Thurn-Albrecht, T. P. Russell, and U. Steiner. 2000. Electrically induced structure formation and pattern transfer. *Nature.* 403:874–877.
21. Hill, S. A., S. Wilson, and A. F. Chambers. 1988. Clonal heterogeneity, experimental metastatic ability, and p21 expression in H-ras-transformed NIH 3T3 cells. *J. Natl. Cancer Inst.* 80:484–490.
22. Owen, J. D., P. J. Ruest, D. W. Fry, and S. K. Hanks. 1999. Induced focal adhesion kinase (FAK) expression in FAK-null cells enhances cell spreading and migration requiring both auto- and activation loop phosphorylation sites and inhibits adhesion-dependent tyrosine phosphorylation of Pyk2. *Mol. Cell. Biol.* 19:4806–4818.
23. Rottner, K., M. Krause, M. Gimona, J. V. Small, and J. Wehland. 2001. Zyxin is not colocalized with vasodilator-stimulated phosphoprotein (VASP) at lamellipodial tips and exhibits different dynamics to vinculin, paxillin, and VASP in focal adhesions. *Mol. Biol. Cell.* 12:3103–3113.
24. Allingham, J. S., R. Smith, and I. Rayment. 2005. The structural basis of blebbistatin inhibition and specificity for myosin II. *Nat. Struct. Mol. Biol.* 4:378–379.

25. Straight, A. F., A. Cheung, J. Limouze, I. Chen, N. J. Westwood, J. R. Sellers, and T. J. Mitchison. 2003. Dissecting temporal and spatial control of cytokinesis with a myosin II inhibitor. *Science*. 299:1743–1747.

26. Guha, M., M. Zhou, and Y. L. Wang. 2005. Cortical actin turnover during cytokinesis requires myosin II. *Curr. Biol.* 15:732–736.

27. Kolega, J. 2004. Phototoxicity and photoinactivation of blebbistatin in UV and visible light. *Biochem. Biophys. Res. Commun.* 320:1020–1025.

28. Sakamoto, T., J. Limouze, C. A. Combs, A. F. Straight, and J. R. Sellers. 2005. Blebbistatin, a myosin II inhibitor, is photoinactivated by blue light. *Biochemistry.* 44:584–588.

29. Dunn, G. A. 1983. Characterising a kinesis response: time averaged measures of cell speed and directional persistence. *Agents Actions Suppl.* 12:14–33.

30. Horwitz, A. R., and J. T. Parsons. 1999. Cell migration—movin' on. *Science*. 286:1102–1103.

31. Braren, R., H. Hu, Y. H. Kim, H. E. Beggs, L. F. Reichardt, and R. Wang. 2006. Endothelial FAK is essential for vascular network stability, cell survival, and lamellipodial formation. *J. Cell Biol.* 172:151–162.

32. Tilghman, R. W., J. K. Slack-Davis, N. Sergina, K. H. Martin, M. Iwanicki, E. D. Hershey, H. E. Beggs, L. F. Reichardt, and J. T. Parsons. 2005. Focal adhesion kinase is required for the spatial organization of the leading edge in migrating cells. *J. Cell Sci.* 118:2613–2623.

33. Berry, C. C., G. Campbell, A. Spadiccino, M. Robertson, and A. S. Curtis. 2004. The influence of microscale topography on fibroblast attachment and motility. *Biomaterials.* 25:5781–5788.

34. Guo, W. H., M. T. Frey, N. A. Burnham, and Y. L. Wang. 2006. Substrate rigidity regulates the formation and maintenance of tissues. *Biophys. J.* 90:2213–2220.

35. Engler, A. J., M. A. Griffin, S. Sen, C. G. Bonnemann, H. L. Sweeney, and D. E. Discher. 2004. Myotubes differentiate optimally on substrates with tissue-like stiffness: pathological implications for soft or stiff microenvironments. *J. Cell Biol.* 166:877–887.

36. Gaudet, C., W. A. Marganski, S. Kim, C. T. Brown, V. Gunderia, M. Dembo, and J. Y. Wong. 2003. Influence of type I collagen surface density on fibroblast spreading, motility, and contractility. *Biophys. J.* 85:3329–3335.

37. Lee, J., A. Ishihara, G. Oxford, B. Johnson, and K. Jacobson. 1999. Regulation of cell movement is mediated by stretch-activated calcium channels. *Nature.* 400:382–386.

38. Munevar, S., Y. L. Wang, and M. Dembo. 2004. Regulation of mechanical interactions between fibroblasts and the substratum by stretch-activated Ca2+ entry. *J. Cell Sci.* 117:85–92.

39. Parsons, J. T. 2003. Focal adhesion kinase: the first ten years. *J. Cell Sci.* 116:1409–1416.